Published in final edited form as:
Optom Vis Sci. 2012 May ; 89(5): 667–677. doi:10.1097/OPX.0b013e31824eeb25.

Foveal Localization in Non-exudative AMD Using Scanning Laser Polarimetry

Dean A. VanNasdale, OD, PhD, FAAO, **Ann E. Elsner, PhD, FAAO**, **Kimberly D. Kohne, OD, FAAO**, **Todd D. Peabody, OD, FAAO**, **Victor E. Malinovsky, OD, FAAO**, **Bryan P. Haggerty, AA**, **Anke Weber, MD**, and **Christopher A. Clark, OD**
Indiana University School of Optometry, Bloomington, Indiana (DAVN, AEE, KDK, TDP, VEM, BPH, CAC), and Aachen University Hospital, Aachen, Germany (AW)

Abstract

Purpose—To determine whether custom scanning laser polarimetry (SLP) images, differing in polarization content, can be used to accurately localize the fovea in the presence of non-exudative age-related macular degeneration (AMD). To determine whether alterations to the foveal structure in non-exudative AMD significantly disrupts the birefringent Henle fiber layer, responsible for the macular cross pattern in some SLP images. To determine whether phase retardation information, specifically color-coded information representing its magnitude and axis, allow better foveal localization than images including retardation amplitude only.

Methods—SLP images were acquired in 25 AMD subjects and 25 age-matched controls. Raw data were used to generate 5 custom image types differing in polarization content. The foveal location was marked by 3 graders in each image type for each subject. The difference in variability was compared between the AMD subjects and matched controls. We further determined whether the orientation of Henle fiber layer phase retardation improved localization in 10 subjects with the highest variability in images including only phase retardation amplitude.

Results—Images that differed in polarization content led to strikingly different visualizations of AMD pathology. The Henle fiber layer remained sufficiently intact to assist in fovea localization in all subjects, but with more variability in the AMD group. For both the AMD and matched control group, images containing birefringence amplitude and orientation information reduced the amount of intra-grader, inter-grader, and inter-image variability for estimating foveal location.

Conclusions—The disruption in Henle fiber birefringence was evident in the eyes with AMD, but nevertheless was sufficient to help in foveal localization despite macular pathology. Phase retardation amplitude and axis of orientation can be a useful tool in foveal localization in patients with AMD.

Keywords

fovea; polarimetry; birefringence; phase retardation; age-related macular degeneration; retina

Age-related macular degeneration (AMD) is responsible for the highest prevalence of vision loss in individuals older than 55 years in industrialized countries.[1,2] AMD is characterized by the widespread accumulation of debris in the outer retina, involving the retinal pigment epithelium (RPE) and Bruch's membrane, along with damage to the overlying

Corresponding author: Dean VanNasdale, Indiana University School of Optometry, 800 E. Atwater Ave, Bloomington, IN 47405, dvannasd@indiana.edu.

Material in this manuscript has been presented previously at the 2010 Association for Research in Vision and Ophthalmology annual meeting in Fort Lauderdale, Florida.

photoreceptors.[3-5] Cone photoreceptor integrity may be sufficient to provide good visual acuity in early AMD, but overall function in the central macula is diminished, demonstrated by abnormally low optical density of the cone photopigments.[6] Significant damage may occur in the deeper retinal structure in early to moderate AMD, while the more superficial retinal axons may remain intact until advanced pathology develops.

Retinal imaging using scanning laser polarimetry (SLP) can be used to differentially emphasize normal structures and pathological features in the retina. Spot scanning, instead of flood illumination, reduces unwanted light scatter and enhances contrast by illuminating and detecting only a small patch of retina at a time as it is scanned in a raster pattern. SLP can achieve high contrast, *en face* retinal images by using a small confocal aperture, which allows only light from a small focal volume to be imaged by the system, eliminating unwanted scatter from objects outside the focal plane. In SLP, a rotating polarization element is used to generate several polarization conditions for light illuminating the retina. These different conditions can be used to generate a series of diverse images from the same raw data set. Structures that cause multiple scattering, such as the RPE, or pathology occurring in the deeper layers of the retina, are visualized easily in images emphasizing light that is depolarized.[7-10] Phase retardation, or birefringence changes, can be used to emphasize the retinal nerve fiber layer,[11-13] the photoreceptor axons in the central macula that constitute the Henle fiber layer,[14-16] and the sclera.[15,17-20] Thus, by selecting specific polarization conditions an image can be formed to emphasize retinal birefringence or features that scatter light, as well as to increase image contrast.[21]

Pathological features associated with macular diseases have been characterized using SLP imaging, including central serous chorioretinopathy,[9] epiretinal membranes,[22] and AMD. Pathological features associated with AMD appear with high contrast in near infrared imaging,[23] and characterization of AMD pathology using SLP includes increased depolarization of hard drusen,[7] improved visualization of pigment clumping,[8] and irregular birefringence changes associated with exudative lesions,[10,24] and retinal fibrosis.[14]

Pathology in the central macula associated with AMD makes localization difficult for features like the fovea, the retinal location responsible for our most acute vision, but localization of pathology relative to the fovea is clinically useful, and has been incorporated into standardized AMD grading schemes.[25] Difficulty in localizing the fovea exists even in normal individuals using traditional methods and becomes more difficult in the presence of retinal disease, where normally highly ordered retinal features may become disrupted or irregular. Methods used to determine the foveal position include relative distance from the optic disc,[26-28] the center of the foveal avascular zone,[26,29] perifoveal capillaries,[30] and the concentration of macular pigments including xanthophyll.[30] The location of a patient's fovea is important when determining the success of treatment, such as intravitreal bevacizumab injection documented by microperimetry,[31] and the extent of retinal disease and impact of treatments on the central macula as documented by optical coherence tomography.[32-34]

The radially symmetric structure of the Henle fiber layer in the central macula can also be used to identify the foveal location, using SLP imaging techniques. The birefringence of the cornea and the Henle fiber layer interact to produce a macular cross pattern centered on the fovea. This pattern has been shown to remain radially symmetric in normal subjects from 1 to 2.5 degrees eccentricity of the center of the macula.[15,35] The macular cross is often still present in patients with advanced exudative AMD, but is more irregular in these patients. The irregularity is correlated with reduced visual acuity,[14] which is consistent with the loss of photoreceptors or other fundus changes that may reduce regular foveal birefringence. The bow tie pattern has been shown to accurately localize the foveal position in normal individuals over a wide range of ages.[16] This technique is potentially useful when foveal

structure is obscured by highly reflective, pathological features in the deeper retinal layers and RPE, or the foveal pit is obscured by retinal thickness changes. In addition to being an intrinsic marker for the position of the central macula, the birefringence pattern of the Henle fiber layer may also act as a surrogate indicator of photoreceptor structure in the presence of pathology associated with AMD.

In this study, we examined custom polarization-sensitive images to localize the fovea in patients with non-exudative AMD. We compared the variability of human graders in foveal localization in AMD patients to that of age-matched controls. We predict that images incorporating birefringence information will demonstrate the least variability, particularly in patients with AMD. Among images containing birefringence information, we hypothesize that images visualizing two components, phase retardation amplitude and orientation, will be more useful in localizing the fovea in significant AMD cases than images that include amplitude only. We also predict that images producing the most variability will be those that have high reflectivity changes or features emphasizing multiple scattering in the deeper retinal structures.

Methods

Subjects

Images were acquired from 25 subjects diagnosed with non-exudative AMD, in 25 eyes (12 right eyes, 13 left eyes). Subjects, 8 males, 17 females, were 56 to 80 years old (average 70.2 + 7.0). All subjects were required to have a complete ophthalmologic examination within the past year that demonstrated retinal pathology associated with AMD. For comparison, images were acquired from 25 subjects with clinically normal retinas, in 25 eyes (12 right eyes, 13 left eyes). The control sample was similar in age and gender, 7 males, 18 females, ranging from 59 to 81 years old (average 69.8 ± 6.5). Control subjects were considered eligible for enrollment if a complete ophthalmologic examination had been completed within the past year, and no signs of ocular pathology were present. Control subjects were also required to have visual acuity of 20/20 or better, unless reduced acuity could be attributed to normal aging lens opacification. Patients with systemic diseases that carry a high likelihood of ocular manifestations were excluded from both groups.

Subjects were recruited from the Indiana University School of Optometry (Bloomington, IN, USA), the Department of Ophthalmology, University Hospital (Aachen, Germany), and the Schepens Eye Institute (Boston, MA, USA) following the human subjects protocol procedures at the respective institutions. Informed consent was obtained from all subjects after explanation of the nature and possible consequences of the study. The research followed the tenets of the Declaration of Helsinki.

Equipment and Procedure

A confocal scanning laser polarimeter (GDx, LaserDiagnostic Technologies/Carl Zeiss Meditec, Dublin, CA) was used to acquire 15 deg × 15 deg images of the macula, as described previously.[7,8,10,14,16,36] The GDx uses a 780-nm linearly polarized light source to scan a raster on the retina. The instrument used in this study has a fixed birefringent element with a magnitude of 60 nm (singlepass retardance) and a fast axis oriented at 15 deg nasally downward to compensate for corneal birefringence.[12] Corneal compensation using this technique is incomplete in most individuals, which results in a macular cross pattern in images demonstrating the birefringence magnitude of the Henle fiber layer. The GDx has 2 detectors, a parallel detector collecting light with the same polarization as the input light; and a crossed detector, collecting light with polarization that is 90 degrees from the input polarization. Each detector produces images at 20 different input polarizations, for a total of

40 images per image series. Each image has 256 × 256 resolution with 8-bit grayscale. The image series has an acquisition time of approximately 0.9 seconds and is performed non-invasively and without mydriasis. When images were acquired, fixation was displaced from the center of the image to eliminate a reflection artifact inherent in the GDx system that could mask the foveal pit and light reflex (Fig. 1). This also ensured that the foveal location would be sufficiently displaced to an unpredictable location to eliminate grading bias.

Raw image data were processed using custom Matlab routines (Matlab, Mathworks, Natick, MA), with five image types used for grading (Fig. 1). These images differ based on polarization content for each pixel over the 20 input polarizations and emphasize different retinal structures resulting from light/tissue interactions.[7-10,14,22,36] The Depolarized Light Image is computed as the minimum value of the modulation for light returning to the crossed detector, which removes any variation due to polarization across the 20 images. This image minimizes features that are visualized via their polarization changes and similarly minimizes specular reflections, while maximizing deeper structures and those that have enhanced contrast from scattered light. RPE changes and regions of atrophy with clearly demarcated borders are emphasized in the Depolarized Light Images. The blood vessel contrast is heightened due to attenuation of light returning from the retinal pigment epithelium, and the vessel distribution can be used to indicate the general region of the fovea. The Confocal Image is polarization insensitive, analogous to a scanning laser ophthalmoscope image, and is computed as the average of the amount of light returning to both the parallel and crossed detectors. This image often looks similar to the Maximum of the Parallel Detector Image unless there is strongly reflecting superficial pathology. The Maximum of the Parallel Detector Image is computed from the highest amplitude of modulation in the parallel detector, regardless of input polarization angle. This image emphasizes more specularly reflected or polarization retaining structures, which are generally located in the more superficial retina.

Other image types have more direct visualization of birefringence information. The Henle fiber layer polarization is visualized as the macular cross pattern in the Birefringence Image, which is computed as the amplitude of the modulation across polarization input angles of the light returning to the crossed detector. This computation demonstrates the phase retardation at each pixel due to the interaction of the birefringence of the cornea and the cone axons in the Henle fiber layer. This grayscale image is limited to showing only the amplitude of the polarization modulation and does not visualize the input polarization conditions that produced the maximum light return, which should vary in a radially symmetric pattern. In comparison, the Maximum Phase of the Crossed Detector Image is a pseudo-color image used to visualize the polarization input condition that produces the maximum light return in the crossed detector at each pixel.[10] The color code for the phase of the maximum amplitude of the crossed detector signal is plotted as a cardinal directions map, in which opponent colors are plotted opposite to each other: red vs. green, blue vs. yellow. The saturation indicates the strength of the signal, with the weaker (least saturated) signal in the center. The visual impact of a weak signal in this image is minimized, and the radially symmetric color pattern localizes the center of the macula to a smaller area than the grayscale birefringence image in normal subjects.[16] To make more equivalent the visibility of the bow tie, we improved the contrast and visualization of the dimmest image types by using the Auto Levels function in Adobe Photoshop (Adobe Photoshop, San Jose, CA), which does not favor any image type.

Additional subjects not included in the statistical analyses were studied separately with spectral domain optical coherence tomography (Spectralis, Heidelberg Engineering, Heidelberg, Germany) to confirm the location and nature of pathology seen in SLP *en face* imaging. The Henle fiber layer, which is superficial to the layers containing drusen and

alterations to Bruch's membrane in AMD, is nevertheless potentially impacted by sufficiently elevated pathology or by the barrier the debris produced beneath the photoreceptors.

Image Grading

The location of the fovea was determined for all subjects at 2 separate times (Time 1 and Time 2) by 3 graders (VM, KK, and TP). With a conversion factor of 1 deg of visual angle per 300 microns at the retina, each pixel is 17.6 microns on the retina.

The variability of foveal localization was compared for patients with AMD vs. control subjects, and for individual image types. The intra-grader distance is the Euclidian distance between the locations for Time1 and Time 2, computed separately for each grader, and then averaged. The inter-grader distance is the average difference between graders, selected pairwise, using the mean location of Time 1 and Time 2.

Intra-grader Variability

To determine the influences on intra-grader variability averaged across the three graders, we performed a repeated measures ANOVA evaluating the influence of image type, subject category (AMD vs. control), and interaction of the two. We also evaluated the influence of image type on the intra-grader variability averaged across graders using planned comparisons between each combination of image type.

Inter-grader Variability

To determine the influences on inter-grader variability averaged across the three grader combinations, we performed a repeated measures ANOVA evaluating the influence of image type, subject category (AMD vs. control), and interaction of the two. We also evaluated the influence of image type on the inter-grader variability averaged across grading combinations using planned comparisons between each combination of image type.

Birefringence with and without Orientation Information

To determine if information from the Maximum of the Crossed Detector Image (magnitude and orientation information about Henle layer birefringence) provided any benefit in localizing the fovea in instances when the Birefringence image (phase retardation magnitude alone) was variable, we examined the 10 subjects with the highest intra-grader variability on the Birefringence Image. In these 10 subjects, we compared the intra-grader variability in the Birefringence Image to the intra-grader variability in the Maximum Phase of the Crossed Detector Image using a paired t-test.

Results

Pathology vs. Matched Control Variability

The macular cross pattern was clearly seen in all subjects despite normal aging changes and pathological features associated with non-exudative AMD (Figs. 2-4). Very different aspects and extents of macular pathology in AMD are visualized by the different image types, yet despite extensive damage, the macular cross pattern remained relatively intact.

Unlike results from the normal subject shown in Fig. 1, the boundaries of the foveal pit were diminished or absent in many subjects, particularly in patients with non-exudative AMD. The 3 corresponding image types in Figs. 2-4 that do not include birefringence information show obvious areas of extensive pathology. The visual acuity for the patient in Fig. 2 was good, 20/30, despite the proximity of pathology to the center of the macula. The pathology

shown in Fig. 2 has numerous focal features in the Depolarized Light Image that is more extensive than what is visible in the Maximum of the Parallel Detector Image, with widespread drusen and RPE defects covering the central 15 deg of the macula. Many of these deeper changes cannot be seen in the Confocal Image. The Maximum of the Parallel Detector Image and the Confocal Image clearly show highly reflective, more superficial damage to the retina. Thus, the foveal location is clearly visible in all image types in Fig. 1, but not in Figs. 2-4. Even in the presence of widespread pathology present in the central macula, the macular cross pattern seen in the Birefringence image remains relatively intact, and remarkably the orientation of the Henle fiber layer is sufficiently regular to produce a number of distinct axes in the Maximum Phase of the Crossed Detector image, allowing very precise localization by the three graders.

The pathological features in Fig. 3 are even more extensive near the fovea, compared with Fig. 2. The grayscale display of the birefringence amplitude in Fig. 3 is insufficient to accurately localize the fovea, because the bowtie is disrupted. The addition of phase information, demonstrated in pseudo-color, better indicates the location of the fovea in this patient.

The amount of disruption to the foveal region can be large and nevertheless the bow tie pattern remains (Fig 4). Further, the small retinal vessels still indicate the general region of the fovea. The Depolarized Light image clearly marks the boundary of the large coalesced druse in the foveal region shown in the spectral domain optical coherence tomography (SDOCT) image. This druse elevates the photoreceptor layers into normally what would be the space occupied by the Henle fiber layer. Reflectivity changes just inferior to the fovea, seen in the Confocal image and the Maximum of the Parallel Detector image, indicate some disruption of the inner retinal layers as well.

Intra-grader Variability

The average intra-grader variability in foveal localization averaged across all image types was 8.8 pixels (154 microns) for the AMD group and 5.1 pixels (89 microns) for the matched controls. Fig. 5 shows the overall intra-grader variability for the two groups categorized by image type. Repeated measures ANOVA analysis showed a significant difference in the main effect of subject category ($p < 0.001$), image type ($p < 0.001$), and the interaction of the two ($p = 0.022$), indicating that it was more difficult to localize the fovea in the patients with AMD, and certain image types allowed more accurate localization for the two groups. Additionally, some image types produced relatively less variable localization in the AMD group than in the control group.

The Depolarized Light Image had the largest intra-grader variability for both groups with an overall average of 13.5 pixels (237 microns) in the AMD group and 8.5 (150 microns) in the control group. Between groups, the largest intra-grader discrepancy was in the Maximum of the Parallel Detector Image. The average intra-grader variability for the Maximum of the Parallel Detector Image was 11.6 pixels (204 microns) in the AMD group and 5.0 pixels (88 microns) in the control group. The smallest discrepancy between the two groups was in the Maximum Phase of the Crossed Detector Image. The average intra-grader variability for the Maximum Phase of the Crossed Detector Image was 3.9 pixels (68 microns) in the AMD group and 2.9 pixels (52 microns) in the control group. Planned comparisons for intra-grader variability within the two groups demonstrate that the image type with the least intra-grader variability, the Maximum Phase of the Crossed Detector Image, was not statistically less variable than the Birefringence Image, but was significantly less variable than the other 3 image types in the AMD group ($p \leq 0.001$). The Birefringence Image was also less variable than the Depolarized Light Image ($p < 0.001$), but not statistically less variable than any of the other image types. For the control group, the Maximum Phase of the Crossed Detector

Image and the Depolarized Light Image were only statistically less variable than the Depolarized Light Image ($p < 0.001$ for each comparison).

Inter-grader Variability

The average inter-grader variability in foveal localization averaged across all image types was 11.0 pixels (193 microns) for the AMD group and 7.3 pixels (129 microns) for the matched controls. Fig. 6 shows the overall inter-grader variability for the two groups categorized by image type. Repeated measures ANOVA analysis showed a significant difference in the main effect of subject category ($p < 0.001$) and image type ($p < 0.001$). That is, it was more difficult to localize the fovea in the patients with AMD than in controls, and certain image types allowed more accurate localization. However, the interaction of the two was not significant ($p = 0.095$), indicating that images types that led to more variable localization of the fovea in control subjects were also less accurate in patients with AMD.

The Confocal Image had the largest inter-grader variability for the AMD group with an overall average of 14.6 pixels (257 microns). The Depolarized Light Image had the largest inter-grader variability for the control group with an overall average of 11.4 pixels (200 microns). Between subject groups, the largest inter-grader discrepancy was in the Confocal Image. The average inter-grader variability for the Confocal Image was 14.6 pixels (257 microns) in the AMD group and 9.3 pixels (122 microns) in the control group. The smallest discrepancy between the two groups was in the Maximum Phase of the Crossed Detector Image. The average inter-grader variability for the Maximum Phase of the Crossed Detector Image was 6.4 pixels (113 microns) in the AMD group and 5.5 pixels (98 microns) in the control group. Planned comparisons for inter-grader variability within the two groups demonstrate that the image type with the least inter-grader variability, the Maximum Phase of the Crossed Detector Image, was not statistically better than the Birefringence Image, but was significantly less variable than the other 3 image types for the AMD group ($p < 0.001$ for each comparison). In the AMD group, the Birefringence Image was also statistically less variable than the Depolarized Light Image and the Confocal Image ($p < 0.001$ for each comparison). For the control group, the Maximum Phase of the Crossed Detector Image, the Birefringence Image, the Maximum of the Parallel Detector Image and the Confocal Image were not statistically less variable than each other, but all were statistically less variable than the Depolarized Light Image ($p < 0.001$ for each comparison).

Birefringence with and without Phase Information

For the 10 subjects in each group with the highest intra-grader variability in the Birefringence image, we investigated the effect of adding color coded phase retardation information to determine whether the fovea could be localized with less variability. The results from the Birefringence image were compared to those from the Maximum Phase of the Crossed Detector Image. The addition of the extra information from the orientation of the phase retardation demonstrated significantly less intra-grader variability than the Birefringence Image for the AMD group (paired t-test, $p = 0.0114$). The Maximum Phase of the Crossed Detector Image did not show a significant benefit in the control group (paired t-test $p = 0.0706$).

Discussion

In this study, we demonstrated extensive pathology in eyes with AMD, yet a sufficiently intact Henle fiber layer remained to produce a macular cross in SLP imaging. For this study we acquired images with an older model GDx that is no longer in production. Unlike more recent models, this particular instrument utilizes a fixed corneal compensating element. Custom images used for analysis were calculated from raw imaging data using custom

software developed by the investigators and their collaborators. We compared the variability in foveal localization in patients with AMD and matched controls using 5 custom SLP images, some of which contain the birefringence information needed to detect the macular cross and others based on light returning from the macula without regard for polarization properties. We evaluated these image types based on intra-grader, inter-grader, and inter-image variability of 3 graders. Variability in each of the 5 image types was higher for the AMD group. However, the 2 image types that incorporated phase retardation changes associated with the Henle fiber layer (the Birefringence Image and the Maximum Phase of the Crossed Detector Image) reduced the variability in both the AMD group and matched controls.

Each of the 2 image types incorporating phase retardation information demonstrate a macular cross pattern centered on the fovea, representing the interaction between the Henle fiber layer birefringence and residual corneal birefringence. Corneal birefringence alone exhibits significant inter-individual variability, both in orientation and magnitude,[37,38] and the instrument used in this study has a fixed polarization element. Consequently, corneal birefringence compensation was incomplete in most subjects.[39] resulting in a unique axis for many individuals in the Birefringence Image and a unique color coding pattern for the Maximum Phase of the Crossed Detector Image. Perfect compensation of the cornea may be unnecessary for this type of analysis and the cross pattern produced by incomplete compensation can still be used to locate the foveal position directly, based on the foveal anatomy. Using polarimetry information does not require additional retinal landmarks, such as a foveal light reflex or macular pigment distribution, which can be irregular and highly variable even in the normal retina, and requires no knowledge of individual differences in corneal birefringence.

Newer commercially available instruments provide complete corneal compensation, customizable for individual patients. The Henle fiber layer is consistent in distribution and phase retardation magnitude in individuals of similar age.[15,35] With full corneal compensation, the Henle fiber layer would be the only structure in these images providing phase retardation information. The resulting images would have different characteristics and would be more similar across subjects. The Birefringence Image would demonstrate a thickness-dependent annular pattern, instead of a cross centered on the fovea, and the Maximum Phase of the Crossed Detector Image would demonstrate a radial spoking pattern, with color coded axes consistent across subjects.

With complete corneal compensation, it is possible that fewer polarization conditions could be used to generate a pattern necessary for foveal localization. Each input condition would generate a unique axis centered on the fovea for normal subjects exhibiting an intact Henle fiber layer. Reducing the number of polarization conditions may be problematic in patients with macular disease however, where irregularity of the Henle fiber layer in unpredictable locations may cause some axes to be irregular and unusable. In these instances, oversampling with a greater number of polarization conditions would be preferable to ensure multiple usable axes.

There is little inter-individual variability in the structural regularity of the normal Henle fiber layer, which does not appreciably change with normal aging, and can persist in the presence of advanced macular disease,[14] and glaucoma.[40] As a result, this technique is potentially more robust than traditional methods currently used clinically. In fact, we found that location variability was nearly identical for the AMD group and matched controls when birefringence information was incorporated. This finding indicates that the Henle fiber layer remains largely intact and can be used as an optical signature for the foveal position in the presence of moderate macular disease. This is consistent with previous findings in patients

with exudative AMD, where 55% of patients with neovascular changes exhibited either a fully or partially intact macular cross pattern, the extent of which was correlated with visual acuity.[14] When considering the 2 image types that contained birefringence information, the Maximum Phase of the Crossed Detector Image showed a significant advantage over the Birefringence Image for AMD subjects in instances when the Birefringence had the highest intra-grader variability. This was expected, as the Maximum Phase of the Crossed Detector Image displays information regarding both the magnitude and orientation of the Henle fiber layer birefringence, giving a more precise marker of foveal location.

The 3 images that did not contain birefringence information had substantially more variability in foveal localization. The Maximum of the Parallel Detector emphasizes highly reflective features, which would include the foveal light reflex. If present, this landmark would be a good indicator of foveal position, but its presence relies on a highly reflective foveal pit with smooth contours. Both conditions are more likely in the control group. Irregularities in the reflective retinal surface that disrupt the contour of the foveal pit are more common in AMD and would likely increase localization variability for this image type. This potentially contributed to the large discrepancy in variability between the two subject groups. Foveal localization using the Confocal Image also demonstrated high variability. The Confocal Image is analogous to a polarization insensitive confocal scanning laser ophthalmoscope image and lacks features typically used to define the foveal position. As with the Maximum of the Parallel Detector Image, the Confocal Image does not emphasize features such as macular pigment distribution, which could be used to get a general estimate of foveal position. Instead, graders had to rely on relative positions of the retinal vasculature to narrow the foveal position for both the Maximum of the Parallel Detector Image and the Confocal Image.

As predicted, the Depolarized Light Image showed significant variability, but this image contains valuable information about multiply scattered light. This type of light/tissue interaction can be used to identify macular pathology, which is emphasized with high contrast. Pathological changes in the Depolarized Light Image have previously been characterized in patients with early AMD changes,[7] central serous chorioretinopathy,[9] and exudative AMD.[10,14,24] Fig. 2 shows the image set that produced the smallest amount of inter-grader variability in the AMD group for the Maximum Phase of the Crossed Detector Image. Even in the presence of significant pathology, a relatively intact macular cross pattern remains in both the Birefringence Image and the Maximum Phase of the Crossed Detector Image, allowing for easy foveal localization. This demonstrates the versatility of SLP imaging, which can be used to localize the fovea, and at the same time provide useful information about pathological changes and irregularities to the normally well-ordered retinal structure.

The diverse image types derived from SLP imaging are powerful tools for assessing pathology associated with AMD. Although all the images used for each subject are derived from a single data set, the individual images demonstrate the complimentary information that displays pathology across the different polarization conditions. Consequently, pathological retinal features are distinguished by different optical signatures. Corresponding locations from the same raw data set can be used measure the relative distance of pathological features from the center of the macula, a factor that is weighted heavily in all major AMD grading protocols. The polarization content in SLP images also provides limited information about the extent and relative depth of pathological features. Polarization preserving changes can be used to isolate more superficial structures, while depolarizing changes can be used to localize deeper features in the retinal changes. This is particularly useful in diseases such as AMD where pathology occurs in the deeper retinal structures initially, leaving much of the superficial structure intact. Fig. 4 is a clear example. The

spectral domain optical coherence tomography image illustrates pathology isolated to the deep retina, while the retina is relatively unaffected superficially. The disruption to the deeper retinal structures are clearly demarcated in the Depolarized Light Image, but poorly defined in the other image types.

Foveal localization using birefringence information does have limitations, particularly in patients with end-stage macular disease. In instances with extensive photoreceptor loss in the central macula, or where the normally symmetric Henle fiber layer becomes sufficiently disrupted, birefringence imaging will no longer show a macular cross.[14] Additionally, collagen from the sclera and exudative changes exhibit birefringent properties, which can obscure the macular cross pattern. Patients with large areas of central geographic atrophy lack the birefringent photoreceptor axons necessary to produce the macular cross pattern and the birefringence signal of the Henle fiber layer may be overwhelmed by the random birefringence associated with the irregular orientation of collagen in the exposed sclera. Similarly, changes associated with neovascularization, fluid leakage, and collagen in fibrotic scarring found in exudative AMD result in a disrupted or irregular bow tie pattern.[14] In either form of end-stage AMD, the lack of a regular radially symmetric macular cross makes foveal localization difficult or impossible.

In this study, we demonstrate that birefringent properties can be used to improve the repeatability and accuracy of foveal localization in patients with AMD. Phase retardation amplitude and orientation information can be used to more precisely localize the fovea when amplitude information alone is insufficient. Foveal localization using SLP imaging is based on the inherent structural properties of the central macula, and does not depend on traditional landmarks, which are absent in the other near infrared polarization sensitive image types. The complementary nature of SLP imaging may have implications for longitudinal studies and clinical trials, where knowledge of advancing or regressing pathology with respect to the center of the fovea is critically important in establishing the efficacy of interventions.

Acknowledgments

This project was support by Grant Numbers K23- EY017886 (DAV), RO1-EY007624 (AEE), RO1-EB002346 (AEE), and P30-EY019008 (SAB) from the National Eye Institute. The content is solely the responsibility of the authors and does not necessarily represent the official views of the National Eye Institute or the National Institutes of Health.

References

1. Klein R, Klein BE, Linton KL. Prevalence of age-related maculopathy. The Beaver Dam Eye Study. Ophthalmology. 1992; 99:933–43. [PubMed: 1630784]
2. Mitchell P, Smith W, Attebo K, Wang JJ. Prevalence of age-related maculopathy in Australia. The Blue Mountains Eye Study. Ophthalmology. 1995; 102:1450–60. [PubMed: 9097791]
3. Hageman GS, Luthert PJ, Victor Chong NH, Johnson LV, Anderson DH, Mullins RF. An integrated hypothesis that considers drusen as biomarkers of immune-mediated processes at the RPE-Bruch's membrane interface in aging and age-related macular degeneration. Prog Retin Eye Res. 2001; 20:705–32. [PubMed: 11587915]
4. Chong NH, Keonin J, Luthert PJ, Frennesson CI, Weingeist DM, Wolf RL, Mullins RF, Hageman GS. Decreased thickness and integrity of the macular elastic layer of Bruch's membrane correspond to the distribution of lesions associated with age-related macular degeneration. Am J Pathol. 2005; 166:241–51. [PubMed: 15632016]
5. Sarks S, Cherepanoff S, Killingsworth M, Sarks J. Relationship of Basal laminar deposit and membranous debris to the clinical presentation of early age-related macular degeneration. Invest Ophthalmol Vis Sci. 2007; 48:968–77. [PubMed: 17325134]

6. Elsner AE, Burns SA, Weiter JJ. Cone photopigment in older subjects: decreased optical density in early age-related macular degeneration. J Opt Soc Am A Opt Image Sci Vis. 2002; 19:215–22. [PubMed: 11778727]
7. Burns SA, Elsner AE, Mellem-Kairala MB, Simmons RB. Improved contrast of subretinal structures using polarization analysis. Invest Ophthalmol Vis Sci. 2003; 44:4061–8. [PubMed: 12939329]
8. Mellem-Kairala MB, Elsner AE, Weber A, Simmons RB, Burns SA. Improved contrast of peripapillary hyperpigmentation using polarization analysis. Invest Ophthalmol Vis Sci. 2005; 46:1099–106. [PubMed: 15728571]
9. Miura M, Elsner AE, Weber A, Cheney MC, Osako M, Usui M, Iwasaki T. Imaging polarimetry in central serous chorioretinopathy. Am J Ophthalmol. 2005; 140:1014–9. [PubMed: 16376644]
10. Elsner AE, Weber A, Cheney MC, VanNasdale DA, Miura M. Imaging polarimetry in patients with neovascular age-related macular degeneration. J Opt Soc Am (A). 2007; 24:1468–80.
11. Dreher AW, Reiter K, Weinreb RN. Spatially resolved birefringence of the retinal nerve fiber layer assessed with a retinal laser ellipsometry. Appl Opt. 1992; 31:3730–5. [PubMed: 20725346]
12. Weinreb RN, Shakiba S, Zangwill L. Scanning laser polarimetry to measure the nerve fiber layer of normal and glaucomatous eyes. Am J Ophthalmol. 1995; 119:627–36. [PubMed: 7733188]
13. Zhou Q, Knighton RW. Light scattering and form birefringence of parallel cylindrical arrays that represent cellular organelles of the retinal nerve fiber layer. Appl Opt. 1997; 36:2273–85. [PubMed: 18253203]
14. Weber A, Elsner AE, Miura M, Kompa S, Cheney MC. Relationship between foveal birefringence and visual acuity in neovascular age-related macular degeneration. Eye (Lond). 2007; 21:353–61. [PubMed: 16397620]
15. Elsner AE, Weber A, Cheney MC, Vannasdale DA. Spatial distribution of macular birefringence associated with the Henle fibers. Vision Res. 2008; 48:2578–85. [PubMed: 18556041]
16. VanNasdale DA, Elsner AE, Weber A, Miura M, Haggerty BP. Determination of foveal location using scanning laser polarimetry. J Vis. 2009; 9:21, 1–17. [PubMed: 19757960]
17. Götzinger E, Pircher M, Baumann B, Hirn C, Vass C, Hitzenberger CK. Analysis of the origin of atypical scanning laser polarimetry patterns by polarization-sensitive optical coherence tomography. Invest Ophthalmol Vis Sci. 2008; 49:5366–72. [PubMed: 19036999]
18. Yamanari M, Lim Y, Makita S, Yasuno Y. Visualization of phase retardation of deep posterior eye by polarization-sensitive swept-source optical coherence tomography with 1-microm probe. Opt Express. 2009; 17:12385–96. [PubMed: 19654640]
19. Miyazawa A, Yamanari M, Makita S, Miura M, Kawana K, Iwaya K, Goto H, Yasuno Y. Tissue discrimination in anterior eye using three optical parameters obtained by polarization sensitive optical coherence tomography. Opt Express. 2009; 17:17426–40. [PubMed: 19907527]
20. Miura M, Yamanari M, Iwasaki T, Itoh M, Yatagai T, Yasuno Y. Polarization-sensitive optical coherence tomography of necrotizing scleritis. Ophthalmic Surg Lasers Imaging. 2009; 40:607–10. [PubMed: 19928731]
21. Bueno JM, Hunter JJ, Cookson CJ, Kisilak ML, Campbell MC. Improved scanning laser fundus imaging using polarimetry. J Opt Soc Am (A). 2007; 24:1337–48.
22. Miura M, Elsner AE, Cheney MC, Usui M, Iwasaki T. Imaging polarimetry and retinal blood vessel quantification at the epiretinal membrane. J Opt Soc Am (A). 2007; 24:1431–7.
23. Elsner AE, Burns SA, Weiter JJ, Delori FC. Infrared imaging of sub-retinal structures in the human ocular fundus. Vision Res. 1996; 36:191–205. [PubMed: 8746253]
24. Miura M, Yamanari M, Iwasaki T, Elsner AE, Makita S, Yatagai T, Yasuno Y. Imaging polarimetry in age-related macular degeneration. Invest Ophthalmol Vis Sci. 2008; 49:2661–7. [PubMed: 18515594]
25. Davis MD, Gangnon RE, Lee LY, Hubbard LD, Klein BE, Klein R, Ferris FL, Bressler SB, Milton RC. The Age-Related Eye Disease Study severity scale for age-related macular degeneration: AREDS Report No. 17. Arch Ophthalmol. 2005; 123:1484–98. Erratum in: Arch Ophthalmol 2006;124:289-90. [PubMed: 16286610]
26. Sunness JS, Gonzalez-Baron J, Applegate CA, Bressler NM, Tian Y, Hawkins B, Barron Y, Bergman A. Enlargement of atrophy and visual acuity loss in the geographic atrophy form of age-related macular degeneration. Ophthalmology. 1999; 106:1768–79. [PubMed: 10485549]

27. Rohrschneider K. Determination of the location of the fovea on the fundus. Invest Ophthalmol Vis Sci. 2004; 45:3257–8. [PubMed: 15326148]

28. Timberlake GT, Sharma MK, Grose SA, Gobert DV, Gauch JM, Maino JH. Retinal location of the preferred retinal locus relative to the fovea in scanning laser ophthalmoscope images. Optom Vis Sci. 2005; 82:177–85. [PubMed: 15767869]

29. Sunness JS, Applegate CA. Long-term follow-up of fixation patterns in eyes with central scotomas from geographic atrophy that is associated with age-related macular degeneration. Am J Ophthalmol. 2005; 140:1085–93. [PubMed: 16376656]

30. Greenstein VC, Santos RA, Tsang SH, Smith RT, Barile GR, Seiple W. Preferred retinal locus in macular disease: characteristics and clinical implications. Retina. 2008; 28:1234–40. [PubMed: 18628727]

31. Ozdemir H, Karacorlu M, Senturk F, Karacorlu SA, Uysal O. Microperimetric changes after intravitreal bevacizumab injection for exudative age-related macular degeneration. Acta Ophthalmol. 2010

32. Emerson GG, Flaxel CJ, Lauer AK, Stout JT, Emerson MV, Nolte S, Wilson DJ, Klein ML. Optical coherence tomography findings during pegaptanib therapy for neovascular age-related macular degeneration. Retina. 2007; 27:724–9. [PubMed: 17621181]

33. Joeres S, Kaplowitz K, Brubaker JW, Updike PG, Collins AT, Walsh AC, Romano PW, Sadda SR. Quantitative comparison of optical coherence tomography after pegaptanib or bevacizumab in neovascular age-related macular degeneration. Ophthalmology. 2008; 115:347–54. [PubMed: 17628685]

34. Leydolt C, Michels S, Prager F, Garhoefer G, Georgopoulos M, Polak K, Schmidt-Erfurth U. Effect of intravitreal bevacizumab (Avastin) in neovascular age-related macular degeneration using a treatment regimen based on optical coherence tomography: 6- and 12-month results. Acta Ophthalmol. 2010; 88:594–600. [PubMed: 19485959]

35. VanNasdale DA, Elsner AE, Hobbs T, Burns SA. Foveal phase retardation changes associated with normal aging. Vision Res. 2011; 51:2263–72. [PubMed: 21893077]

36. Weber A, Cheney M, Smithwick Q, Elsner A. Polarimetric imaging and blood vessel quantification. Opt Express. 2004; 12:5178–90. [PubMed: 19484075]

37. Greenfield DS, Knighton RW. Stability of corneal polarization axis measurements for scanning laser polarimetry. Ophthalmology. 2001; 108:1065–9. [PubMed: 11382630]

38. Weinreb RN, Bowd C, Greenfield DS, Zangwill LM. Measurement of the magnitude and axis of corneal polarization with scanning laser polarimetry. Arch Ophthalmol. 2002; 120:901–6. [PubMed: 12096960]

39. Zhou Q, Weinreb RN. Individualized compensation of anterior segment birefringence during scanning laser polarimetry. Invest Ophthalmol Vis Sci. 2002; 43:2221–8. [PubMed: 12091420]

40. Bagga H, Greenfield DS, Feuer WJ. Quantitative assessment of atypical birefringence images using scanning laser polarimetry with variable corneal compensation. Am J Ophthalmol. 2005; 139:437–46. [PubMed: 15767051]

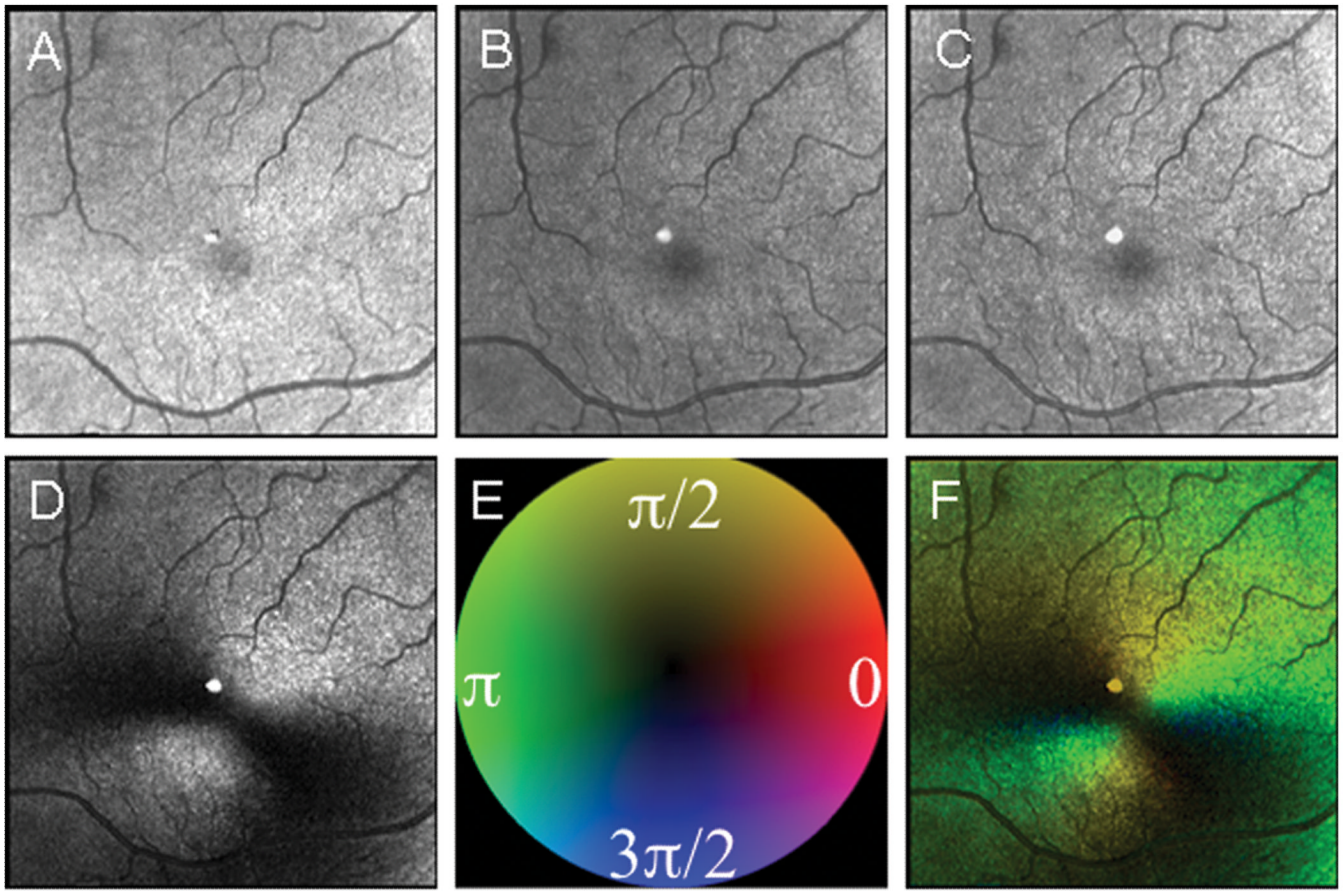

Figure 1.

Five image types used for foveal grading in a 67 year old control subject. **(A)** The Depolarized Light Image. **(B)** The Confocal Image. **(C)** The Maximum of the Parallel Detector Image. **(D)** The Birefringence Image. **(E)** Color Code for Phase of the Maximum Amplitude of the Crossed Detector Signal, as in Elsner et al. (2007). **(F)** The Maximum Phase of the Crossed Detector Image. The two bottom images differ in that the left one lacks phase information and the right one has color coded phase information indicating both the amount of and orientation of birefringence, coded with the cardinal directions color map. There is a bright reflection artifact inherent in this GDx instrument that is at the center of each image. Due to a distinct boundary of the foveal pit in this subject, there is little difference in the repeatability of foveal localization among image types based, with intra-grader variability of 97.3, 54.2, 53.6, 60.5, 50.2 microns, respectively.

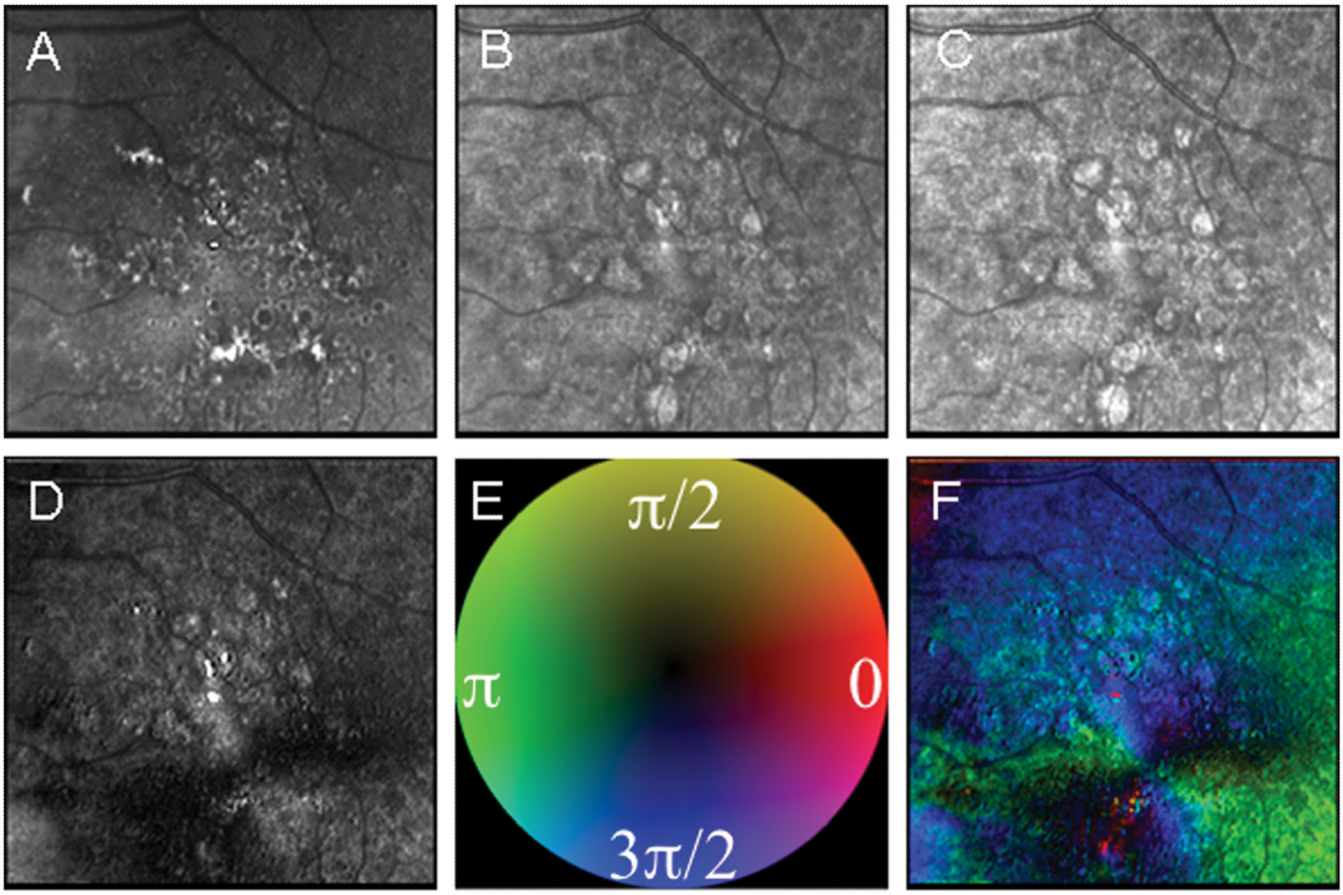

Figure 2.

Example of significant fundus changes due to AMD and the improvement in foveal localizations in some image types compared with others. Using two components to visualize the bow tie pattern, birefringence amplitude and orientation improved localization over the grayscale image types. As above, the five images differ in polarization content. **(A)** The Depolarized Light Image, with the least polarization content, emphasizes the pathology of non-exudative AMD. **(B)** The Confocal Image and **(C)** The Parallel Detector Image, do not have features that appreciably aid in the localization of the fovea. **(D)** The Birefringence Image contains only amplitude information represented in grayscale, which improves, but does not maximize the localization of the fovea. **(E)** Color Code for Phase of the Maximum Amplitude of the Crossed Detector Signal as above. **(F)** The Maximum Phase of the Crossed Detector Image, which shows the amplitude information as saturation and phase as hue, clearly demarcates the fovea center. The average intra-grader variability from the Depolarized Image to the Maximum Phase of the Crossed Detector Image was 214.2, 320.1, 219.9, 100.5, and 81.5 microns, respectively.

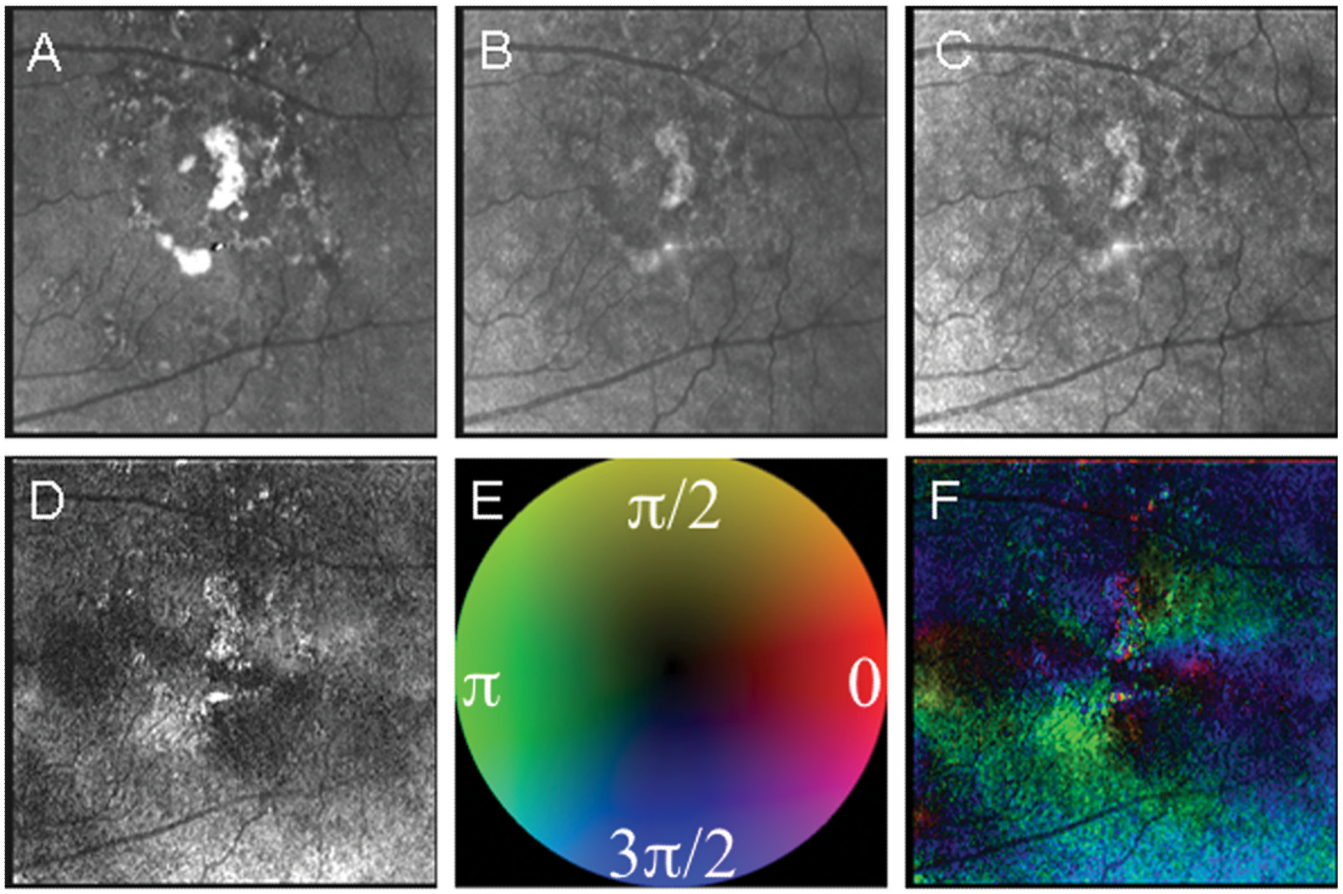

Figure 3.

Example of significant fundus changes due to AMD with even more relative improvement found for foveal localization in the Maximum Phase of the Crossed Detector Image, which gives color coded information about both amplitude and phase of the macular birefringence. **(A)** The Depolarized Light Image, with the least polarization content, emphasizes the pathology of non-exudative AMD. **(B)** The Confocal Image and **(C)** The Parallel Detector Image, do not have features that appreciably aid in the localization of the fovea. **(D)** The Birefringence Image contains only amplitude information represented in grayscale, but the bow tie pattern is disrupted and does not provide optimal information for localization of the fovea. **(E)** Color Code for Phase of the Maximum Amplitude of the Crossed Detector Signal as above. **(F)** The Maximum Phase of the Crossed Detector Image again clearly demarcates the fovea center despite the macular pathology. The average intra-grader variability from the Depolarized Image to the Maximum Phase of the Crossed Detector Image was 159.5, 324.5, 272.4, 186.1, and 27.3 microns, respectively.

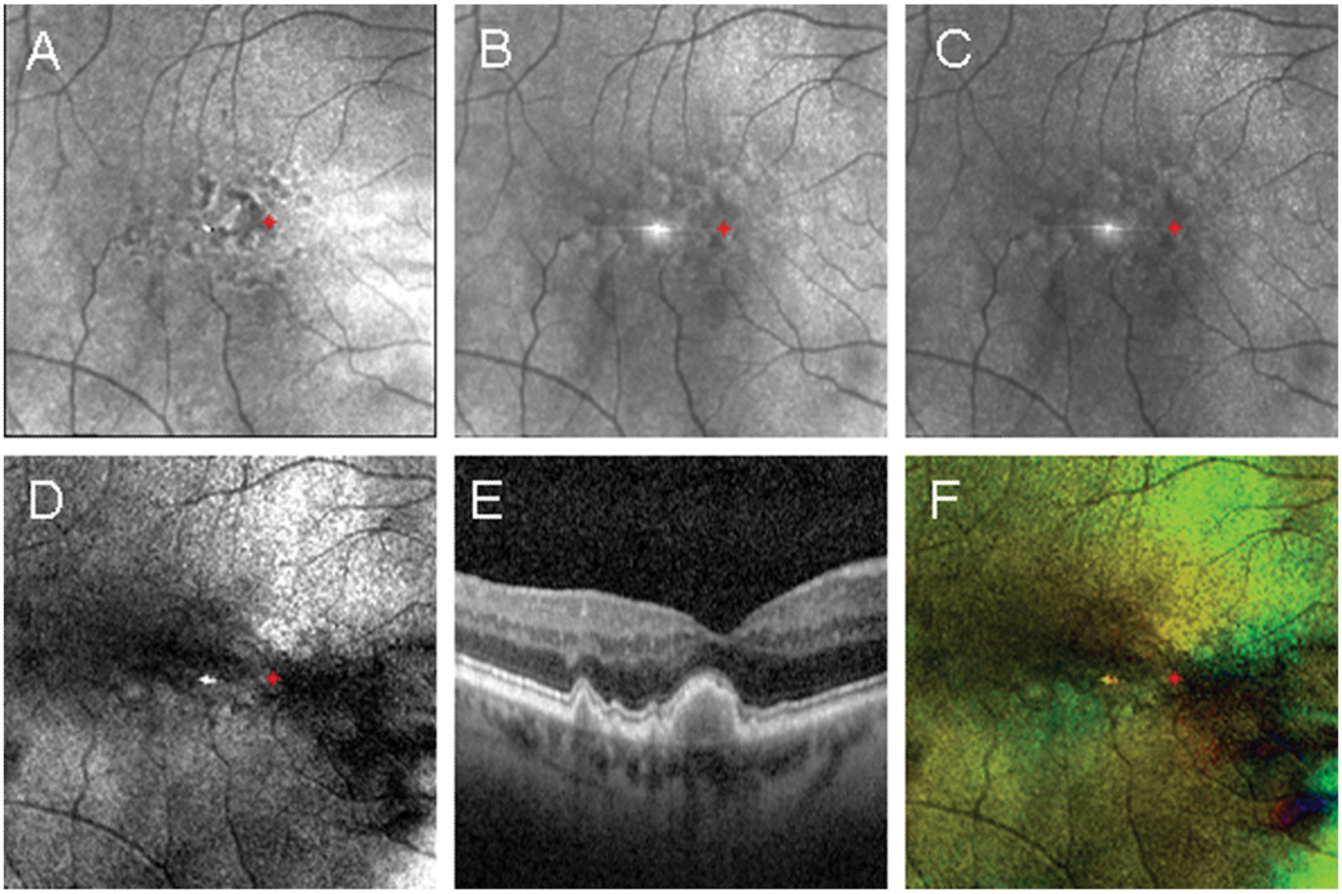

Figure 4.

Example of foveal localization in a subject with large coalesced drusen in the central macula confirmed using spectral domain optical coherence tomography. The red asterisk indicates the foveal location determined using the Maximum Phase of the Crossed Detector Image. Foveal coordinates were then plotted on the remaining images derived from the same raw data set. **(A)** The Depolarized Light Image, with the least polarization content, emphasizes the pathology in the outer retina. **(B)** The Confocal Image and **(C)** The Parallel Detector Image, do not have features that appreciably aid in the localization of the fovea. **(D)** The Birefringence Image contains only amplitude information represented in grayscale, but the macular cross pattern is disrupted and does not provide optimal information for foveal localization. **(E)** The SDOCT image shows the location of pathological features emphasized in the Depolarized Light Image. (F) The Maximum Phase of the Crossed Detector Image, color code as above, again clearly demarcates the fovea center despite central macular pathology.

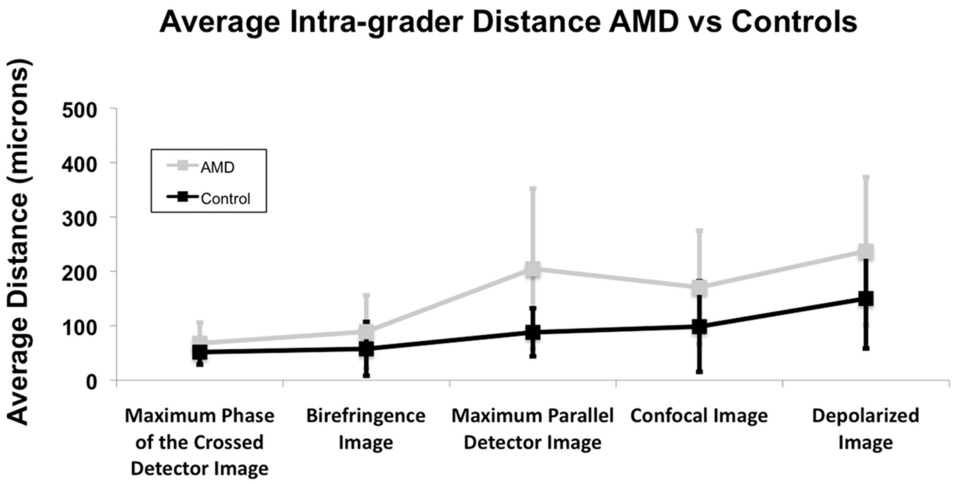

Figure 5.

The overall intra-grader variability for the 3 graders separated by image type for both the AMD and control group. The control group had less variability than the AMD group for each of the different image types. Paired t-test comparing the variability between the AMD group and the control group for each graded image demonstrated significantly more overall variability in the AMD group ($p<0.001$).

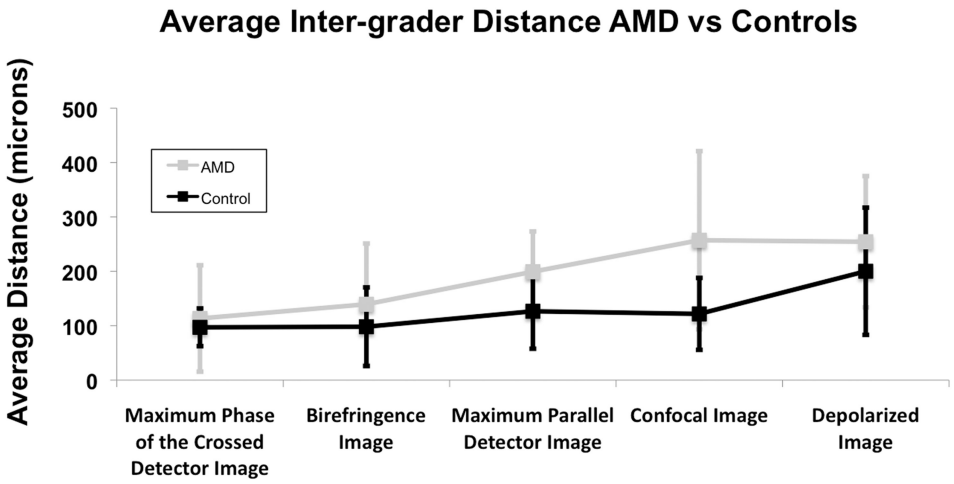

Figure 6.

The overall inter-grader variability for the 3 graders separated by image type for both the AMD and control group. The control group had less variability than the AMD group for each of the different image types. Paired t-test comparing the variability between the AMD group and the control group for each graded image demonstrated significantly more overall variability in the AMD group ($p<0.001$).